Search for a light CP-odd Higgs boson decaying into a pair of τ-leptons in the full ATLAS Run 2 dataset

Manuel Gutsche on behalf of the ATLAS Collaboration
Institute of Nuclear and Particle Physics, TU Dresden

Higgs Hunting 2024
Paris, September 24, 2024

Motivation

- Model independent search: extend search for new Higgs bosons to low masses in unexplored phase space

- Model dependent search: deviation in anomalous magnetic moment of the muon a_μ between experiment and SM prediction [1–7]
- Flavour-aligned two-Higgs-doublet model

  $\Rightarrow$ One SM-like Higgs boson h and additional Higgs bosons $H^\pm$, H, A

  $\Rightarrow$ A CP-odd and could have $m_A < m_h$
- Free parameters such as masses and couplings ζ:

  $\Rightarrow$ Experimentally constrained: Up-type quarks: $\zeta_\mathrm{u} < 0.5$, Down-type quarks: $\zeta_\mathrm{d} < \mathcal{O}(1)$

  $\Rightarrow$ Deviation explained for large lepton couplings $\zeta_\ell \approx 50$ & light A [8]

  $\Rightarrow$ This search: mass hypotheses m_A between 20 GeV and 90 GeV

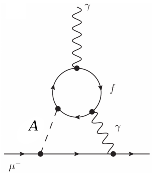

Signal process

- Production of A via gluon fusion and top quark loop
- Cross-sections calculated via ggHiggs [9–20]
- Decay 100 % to τ-lepton pairs
- Limited to leptonic channels because of trigger thresholds

  $\Rightarrow$ Mainly boosted topology

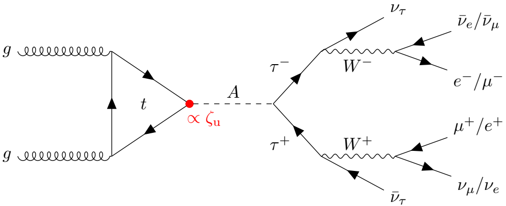

- Restriction to electron-muon final state to reject $Z \to e^+e^-$, $Z \to \mu^+\mu^-$ events

Background processes

- Largest background is $Z/\gamma^* + \text{jets} \rightarrow \tau^+\tau^-$
- Fake lepton background:
  - ⇒ Particles reconstructed as prompt leptons, but are e.g. misidentified jets
  - ⇒ Not well modeled by Monte Carlo
  - ⇒ Estimated via data-driven matrix method [21]
- Other MC backgrounds

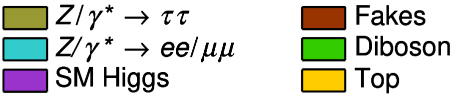

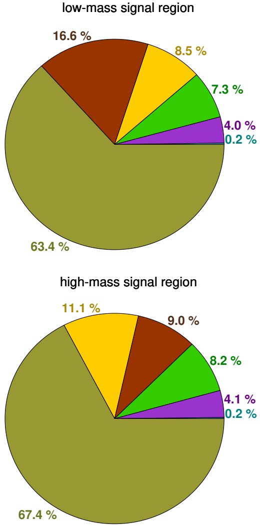

Selection criteria

- One electron and one muon, opposite charge
- `Medium` ID and `Tight` isolation
- Electron:
  $p_{\mathrm{T}}^{e} > 7\,\mathrm{GeV}$, $|\eta_e| < 2.47$, $|\eta_e| \notin (1.37, 1.52)$
  muon:
  $p_{\mathrm{T}}^{\mu} > 7\,\mathrm{GeV}$, $|\eta_\mu| < 2.7$
- Overlap removal prioritizing muons over electrons over jets

Three electron-muon triggers

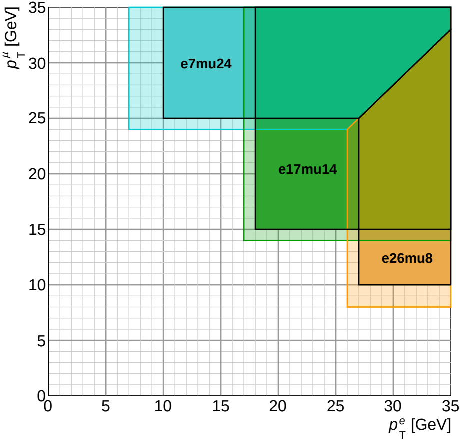

Selection cuts defining regions

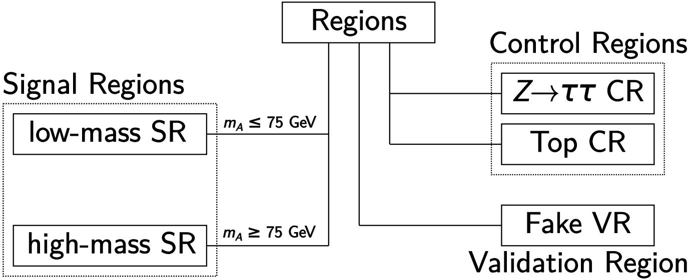

- High missing transverse momentum $E_{\mathrm{T}}^{\mathrm{miss}}$
  - $\Rightarrow$ Expecting neutrinos
- Low transverse mass[a] $m_{\mathrm{T}}^{\mathrm{tot}}$
  - $\Rightarrow$ Diboson & top suppression
- Low angular separation[b] $\Delta R_{\ell\ell}$
  - $\Rightarrow$ Decay topology of CP-odd A boson
- No b-tagged jets
  - $\Rightarrow$ Top suppression

[a] $m_{\mathrm{T}}^{\mathrm{tot}} = \sqrt{\left(p_{\mathrm{T}}^{e} + p_{\mathrm{T}}^{\mu} + E_{\mathrm{T}}^{\mathrm{miss}}\right)^2 - \left(\vec{p}_{\mathrm{T}}^{e} + \vec{p}_{\mathrm{T}}^{\mu} + \vec{E}_{\mathrm{T}}^{\mathrm{miss}}\right)^2}$

[b] $\Delta R_{\ell\ell} = \sqrt{(\Delta\Phi_{\ell\ell})^2 + (\Delta\eta_{\ell\ell})^2}$

Signal regions

Low-mass SR

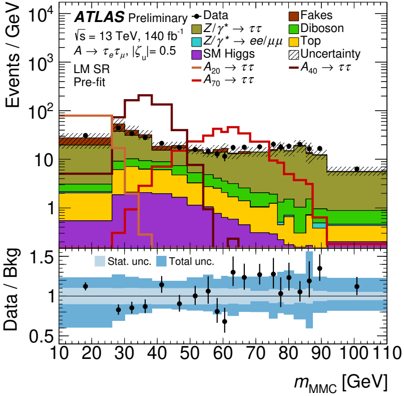

High-mass SR

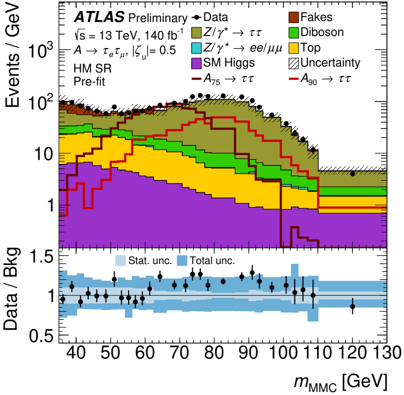

⇒ m_{MMC} is Higgs mass reconstructed via Missing Mass Calculator, which estimates neutrino kinematics with likelihood approach

$Z \to \tau\tau$ control region

- Separated from SR by requiring large $\Delta R_{\ell\ell}$
- Validate $Z \to \tau^+\tau^-$ background modeling
- Reweight $Z \to \tau^+\tau^-$ MC in dependence on n_{jets} within systematic uncertainties
- Used as control region for fit

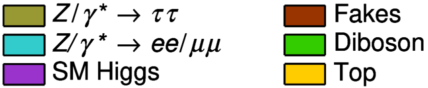

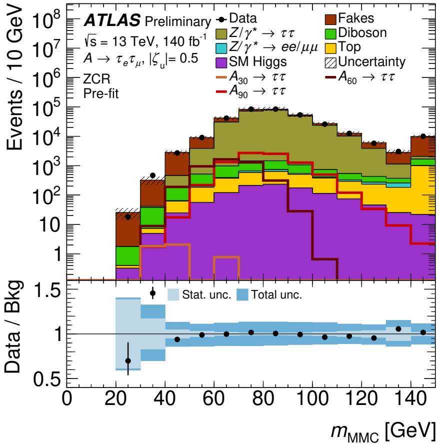

$Z \to \tau\tau$ control region

- Separated from SR by requiring large $\Delta R_{\ell\ell}$
- Validate $Z \to \tau^+\tau^-$ background modeling
- Reweight $Z \to \tau^+\tau^-$ MC in dependence on n_{jets} within systematic uncertainties
- Used as control region for fit

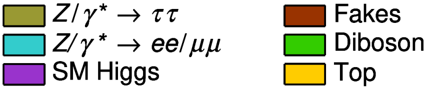

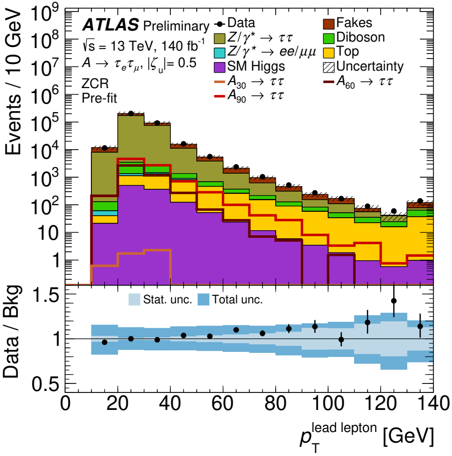

$Z \to \tau\tau$ control region

- Separated from SR by requiring large $\Delta R_{\ell\ell}$
- Validate $Z \to \tau^+\tau^-$ background modeling
- Reweight $Z \to \tau^+\tau^-$ MC in dependence on n_{jets} within systematic uncertainties
- Used as control region for fit

$Z/\gamma^* \to \tau\tau$ | Fakes
$Z/\gamma^* \to ee/\mu\mu$ | Diboson
SM Higgs | Top

before reweighting

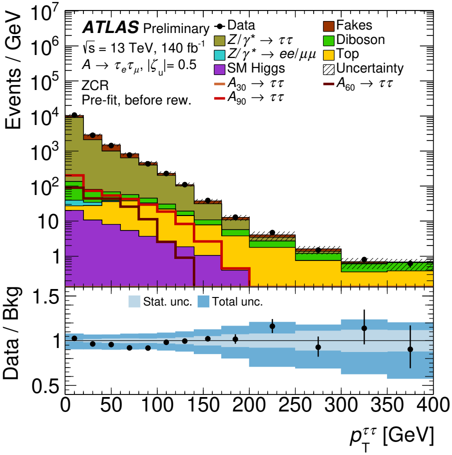

$Z \to \tau\tau$ control region

- Separated from SR by requiring large $\Delta R_{\ell\ell}$
- Validate $Z \to \tau^+\tau^-$ background modeling
- Reweight $Z \to \tau^+\tau^-$ MC in dependence on n_{jets} within systematic uncertainties
- Used as control region for fit

$Z/\gamma^* \to \tau\tau$ | Fakes
$Z/\gamma^* \to ee/\mu\mu$ | Diboson
SM Higgs | Top

after reweighting

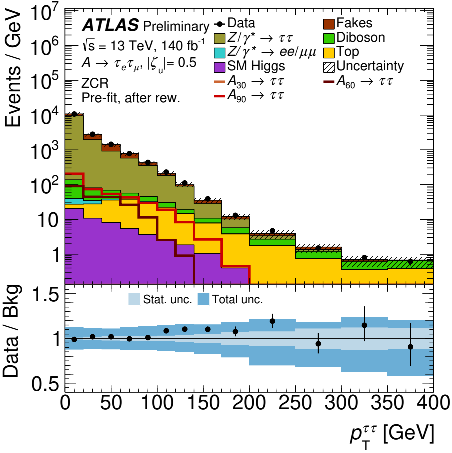

Fake validation region

- Same cuts as $Z \to \tau\tau$ CR, except $q_e \times q_\mu = 1$
- Estimate fake lepton background via data-driven matrix method
- Validate fake lepton background modeling

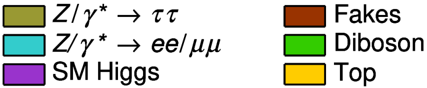

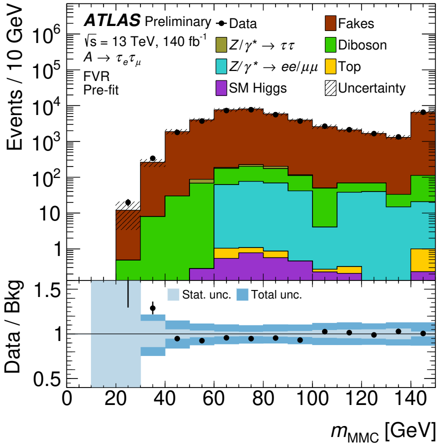

Fake validation region

- Same cuts as $Z \to \tau\tau$ CR, except $q_e \times q_\mu = 1$
- Estimate fake lepton background via data-driven matrix method
- Validate fake lepton background modeling

$Z/\gamma^* \to \tau\tau$ | Fakes
$Z/\gamma^* \to ee/\mu\mu$ | Diboson
SM Higgs | Top

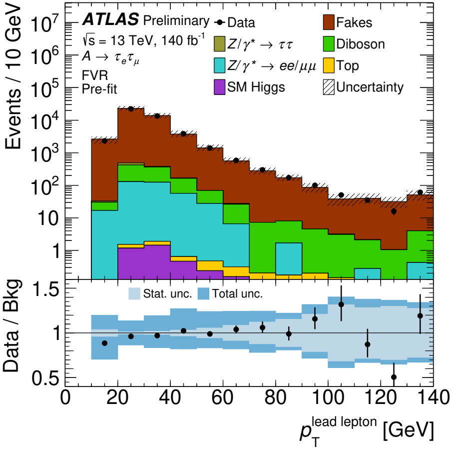

Top control region

- Separated from SR by requiring at least 2 *b*-jets
- Validate top background modeling
- Used as control region for fit

$Z/\gamma^* \to \tau\tau$ Fakes
$Z/\gamma^* \to ee/\mu\mu$ Diboson
SM Higgs Top

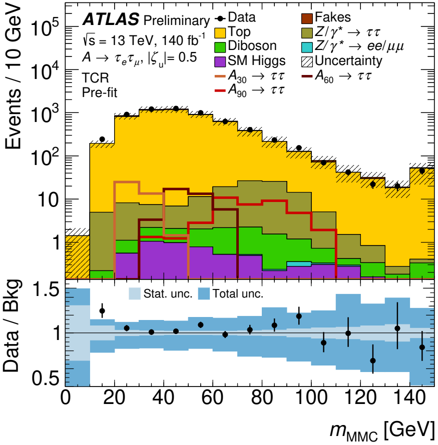

Top control region

- Separated from SR by requiring at least 2 *b*-jets
- Validate top background modeling
- Used as control region for fit

$Z/\gamma^* \to \tau\tau$ | Fakes
$Z/\gamma^* \to ee/\mu\mu$ | Diboson
SM Higgs | Top

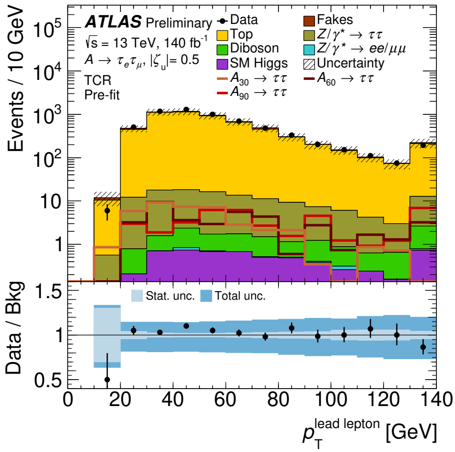

Systematics

- Experimental systematics on efficiencies, detector calibration, missing transverse momentum, pileup reweighting, luminosity
- Uncertainties of MC samples
  - ⇒ Cross-section uncertainties
  - ⇒ Generator uncertainties for $Z \rightarrow \tau^+\tau^-$, Top, Diboson, Signal
- Uncertainties of fake background modeling
  - ⇒ Statistical uncertainty of efficiencies, parametrizations, composition
- Uncertainties of $Z \rightarrow \tau^+\tau^-$ reweighting

Systematic uncertainties on signal strength

Category ($m_A = 20$ GeV)	Relative contrib. to $\Delta\mu$
Data statistical	42%
Systematic	91%
Background statistical	81%
$Z \to \tau^+\tau^-$ statistical	75%
Fake lepton statistical	30%
Other background statistical	7%
Fake lepton systematic	37%
Signal modeling	11%
$Z \to \tau^+\tau^-$ modeling	10%
Muon efficiencies	8%
Diboson modeling	8%
Flavor tagging	5%
Signal statistical	5%
...	

Category ($m_A = 90$ GeV)	Relative contrib. to $\Delta\mu$
Data statistical	10%
Systematic	99%
Background statistical	67%
$Z \to \tau^+\tau^-$ statistical	48%
Fake lepton statistical	47%
Other background statistical	8%
$Z \to \tau^+\tau^-$ reweighting	55%
Signal statistical	51%
Fake lepton systematic	47%
$Z \to \tau^+\tau^-$ modeling	45%
$Z \to \tau^+\tau^-$ and $t\bar{t}$ normalization	34%
$t\bar{t}$ modeling	14%
Flavor tagging	14%
...	

Results

- No significant deviation of the data from SM background expectation observed
- Determine upper limit on $\sigma(gg \to A) \times B(A \to \tau^+\tau^-)$
- Binned likelihood fit of m_{MMC} distribution for each mass hypothesis
- Asymptotic CLs method

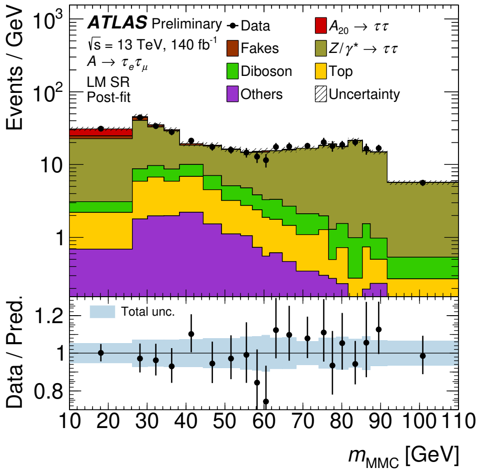

Results

- No significant deviation of the data from SM background expectation observed
- Determine upper limit on $\sigma(gg \rightarrow A) \times B(A \rightarrow \tau^+\tau^-)$
- Binned likelihood fit of m_{MMC} distribution for each mass hypothesis
- Asymptotic CLs method

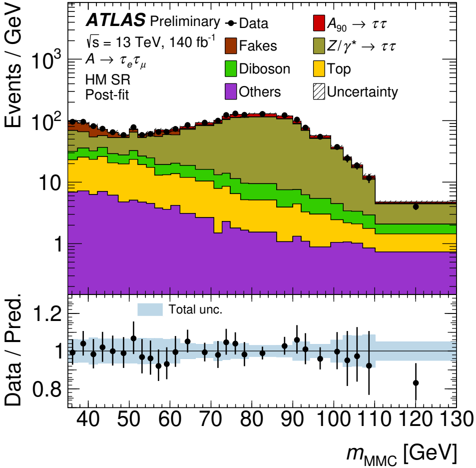

Expected and observed exclusion limits

- Limit set on $\sigma(gg \to A) \times B(A \to \tau^+\tau^-)$
- Transition from low-mass SR to high-mass SR at $m_A = 75\,\mathrm{GeV}$
- Mass range between $20\,\mathrm{GeV}$ and $60\,\mathrm{GeV}$ explored for the first time for this production and decay mode

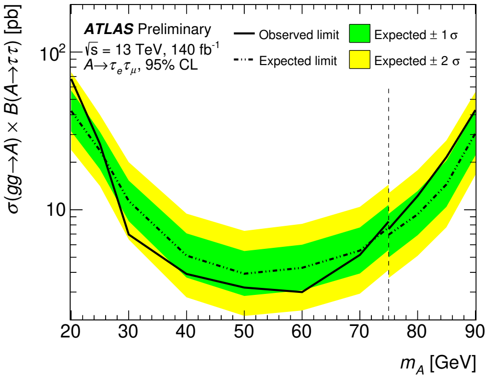

TECHNISCHE UNIVERSITÄT DRESDEN
INSTITUTE OF NUCLEAR AND PARTICLE PHYSICS
FSP Erforschung von Universum und Materie
GEFÖRDERT VOM Bundesministerium für Bildung und Forschung
ATLAS EXPERIMENT

Expected and observed exclusion limits

- Limit set on $|\zeta_{\mathrm{u}}|$
- Transition from low-mass SR to high-mass SR at $m_A = 75\,\mathrm{GeV}$
- This search improves on current upper limit of $|\zeta_{\mathrm{u}}| < 0.5$ [8] over the full mass range

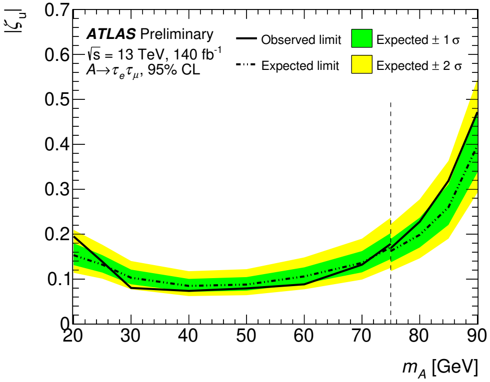

Summary

- Low-mass $A \to \tau^+\tau^-$ search in $e - \mu$ channel
- No significant excess
  - $\Rightarrow$ largest deviation from SM prediction at $20\,\mathrm{GeV}$ with $1.8\,\sigma$
- Exclusion limits set for gluon-fusion production of A boson with decay to $\tau^+\tau^-$:
  - $\Rightarrow$ First limits for $20\,\mathrm{GeV} \leq m_A < 60\,\mathrm{GeV}$
  - $\Rightarrow$ $3.0\,\mathrm{pb}$ to $67.5\,\mathrm{pb}$ for $\sigma(gg \to A) \times B(A \to \tau^+\tau^-)$
  - $\Rightarrow$ 0.074 to 0.47 for $|\zeta_\mathrm{u}|$

$\Rightarrow$ Future reference

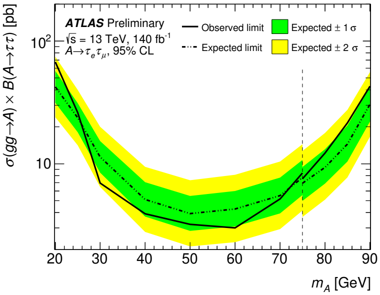

References I

[1] T. Aoyama *et al.*, *The anomalous magnetic moment of the muon in the standard model*, Physics Reports **887** 2020 1 1, 2020, The anomalous magnetic moment of the muon in the Standard Model. [Online]. Available: https://www.sciencedirect.com/science/article/pii/S0370157320302556 (cit. on p. 2).

[2] Muon $g-2$ Collaboration, B. Abi, *et al.*, *Measurement of the positive muon anomalous magnetic moment to 0.46 ppm*, Phys. Rev. Lett. **126** 14 2021 141801 141801, 14 2021. [Online]. Available: https://link.aps.org/doi/10.1103/PhysRevLett.126.141801 (cit. on p. 2).

[3] Muon $g-2$ Collaboration, D. P. Aguillard, *et al.*, *Measurement of the positive muon anomalous magnetic moment to 0.20 ppm*, Phys. Rev. Lett. **131** 16 2023 161802 161802, 16 2023. [Online]. Available: https://link.aps.org/doi/10.1103/PhysRevLett.131.161802 (cit. on p. 2).

[4] G. Colangelo *et al.*, *Prospects for precise predictions of a_μ in the Standard Model*, 2022, 2022. arXiv: 2203.15810 [hep-ph] (cit. on p. 2).

References II

[5] S. Borsanyi *et al.*, *Leading hadronic contribution to the muon magnetic moment from lattice QCD*, Nature **593** 2021 51 51, 2021. [Online]. Available: https://doi.org/10.1038%2Fs41586-021-03418-1 (cit. on p. 2).

[6] A. Boccaletti *et al.*, *High precision calculation of the hadronic vacuum polarisation contribution to the muon anomaly*, 2024, 2024. arXiv: 2407.10913 [hep-lat]. [Online]. Available: https://arxiv.org/abs/2407.10913 (cit. on p. 2).

[7] CMD-3 Collaboration, F. V. Ignatov, *et al.*, *Measurement of the $e^+e^- \to \pi^+\pi^-$ cross section from threshold to 1.2 gev with the cmd-3 detector*, Phys. Rev. D **109** 11 2024 112002 112002, 11 2024. [Online]. Available: https://link.aps.org/doi/10.1103/PhysRevD.109.112002 (cit. on p. 2).

[8] A. Cherchiglia, D. Stöckinger, and H. Stöckinger-Kim, *Muon $g-2$ in the 2hdm: Maximum results and detailed phenomenology*, Phys. Rev. D **98** 3 2018 035001 035001, 3 2018. [Online]. Available: https://link.aps.org/doi/10.1103/PhysRevD.98.035001 (cit. on pp. 2, 21).

References III

[9] R. D. Ball, M. Bonvini, S. Forte, S. Marzani, and G. Ridolfi,
Higgs production in gluon fusion beyond nnlo, Nuclear Physics B **874** 2013 746 746, 2013,
ISSN: 0550-3213. [Online]. Available: http://dx.doi.org/10.1016/j.nuclphysb.2013.06.012
(cit. on p. 3).

[10] M. Bonvini, R. D. Ball, S. Forte, S. Marzani, and G. Ridolfi,
Updated higgs cross section at approximate n3lo,
Journal of Physics G: Nuclear and Particle Physics **41** 2014 095002 095002, 2014, ISSN: 1361-6471.
[Online]. Available: http://dx.doi.org/10.1088/0954-3899/41/9/095002 (cit. on p. 3).

[11] M. Bonvini, S. Marzani, C. Muselli, and L. Rottoli,
On the higgs cross section at n3lo+n3ll and its uncertainty,
Journal of High Energy Physics **2016** 2016, 2016, ISSN: 1029-8479.
[Online]. Available: http://dx.doi.org/10.1007/JHEP08(2016)105 (cit. on p. 3).

[12] T. Ahmed *et al.*, *Pseudo-scalar higgs boson production at $n^3lo_{\mathrm{A}} + n^3ll'$*,
The European Physical Journal C **76** 2016, 2016, ISSN: 1434-6052.
[Online]. Available: http://dx.doi.org/10.1140/epjc/s10052-016-4510-1 (cit. on p. 3).

References IV

[13] M. Bonvini and S. Marzani, *Double resummation for higgs production*, Physical Review Letters **120** 2018, 2018, ISSN: 1079-7114. [Online]. Available: http://dx.doi.org/10.1103/PhysRevLett.120.202003 (cit. on p. 3).

[14] M. Bonvini, *An approximate n3lo cross section for higgs production in gluon fusion*, EPJ Web of Conferences **60** 2013 12008, M. Bosman, A. Juste, M. Martínez, I. Riu, and V. Sorin, Eds. 12008, 2013, ISSN: 2100-014X. [Online]. Available: http://dx.doi.org/10.1051/epjconf/20136012008 (cit. on p. 3).

[15] R. V. Harlander and W. B. Kilgore, *Next-to-next-to-leading order higgs production at hadron colliders*, Physical Review Letters **88** 2002, 2002, ISSN: 1079-7114. [Online]. Available: http://dx.doi.org/10.1103/PhysRevLett.88.201801 (cit. on p. 3).

[16] R. V. Harlander and K. J. Ozeren, *Finite top mass effects for hadronic higgs production at next-to-next-to-leading order*, Journal of High Energy Physics **2009** 2009 088 088, 2009, ISSN: 1029-8479. [Online]. Available: http://dx.doi.org/10.1088/1126-6708/2009/11/088 (cit. on p. 3).

References V

[17] R. V. Harlander, H. Mantler, S. Marzani, and K. J. Ozeren, *Higgs production in gluon fusion at next-to-next-to-leading order qcd for finite top mass*, The European Physical Journal C **66** 2010 359 359, 2010, ISSN: 1434-6052. [Online]. Available: http://dx.doi.org/10.1140/epjc/s10052-010-1258-x (cit. on p. 3).

[18] C. Anastasiou *et al.*, *Higgs boson gluon-fusion production beyond threshold in n3lo qcd*, 2014, 2014. arXiv: 1411.3584 [hep-ph]. [Online]. Available: https://arxiv.org/abs/1411.3584 (cit. on p. 3).

[19] C. Anastasiou *et al.*, *High precision determination of the gluon fusion higgs boson cross-section at the lhc*, 2016, 2016. arXiv: 1602.00695 [hep-ph]. [Online]. Available: https://arxiv.org/abs/1602.00695 (cit. on p. 3).

[20] B. Mistlberger, *Higgs boson production at hadron colliders at n3lo in qcd*, Journal of High Energy Physics **2018** 2018, 2018, ISSN: 1029-8479. [Online]. Available: http://dx.doi.org/10.1007/JHEP05(2018)028 (cit. on p. 3).

References VI

[21] ATLAS Collaboration, *Estimation of non-prompt and fake lepton backgrounds in final states with top quarks produced in proton–proton collisions at* $\sqrt{s} = 8$ *TeV with the ATLAS Detector*, ATLAS-CONF-2014-058, 2014. [Online]. Available: https://cds.cern.ch/record/1951336 (cit. on p. 4).

BACKUP

Selection criteria

		SR Low-mass 20 to 75 GeV	SR High-mass 75 to 90 GeV	Top CR	$Z \to \tau\tau$ CR	Fake VR
E_T^{miss} cut	E_T^{miss}	> 50 GeV	> 30 GeV	> 30 GeV	–	–
Mass cut[1]	m_T^{tot}	< 45 GeV	< 65 GeV	< 65 GeV	< 65 GeV	< 65 GeV
Angular cut[2]	ΔR_{ll}	< 0.7	< 1.0	< 1.0	> 1.4	> 1.4
MMC cut	m_{MMC}	> 0 GeV	> 35 GeV & < 130 GeV	> 0 GeV	> 0 GeV & < 130 GeV	> 0 GeV & < 130 GeV
***b*-tag**	n_{b-jets}	0	0	> 1	0	0
Charge cut	$q_e \times q_\mu$	-1	-1	-1	-1	1

[1] $m_T^{tot} = \sqrt{\left(p_T^e + p_T^\mu + E_T^{miss}\right)^2 - \left(\vec{p}_T^{\,e} + \vec{p}_T^{\,\mu} + \vec{E}_T^{miss}\right)^2}$, [2] $\Delta R = \sqrt{(\Delta\Phi)^2 + (\Delta\eta)^2}$

Observed p_0 value

- Transition from low-mass SR to high-mass SR at $m_A = 75\,\mathrm{GeV}$
- largest deviation from SM prediction at $20\,\mathrm{GeV}$ with $1.8\,\sigma$

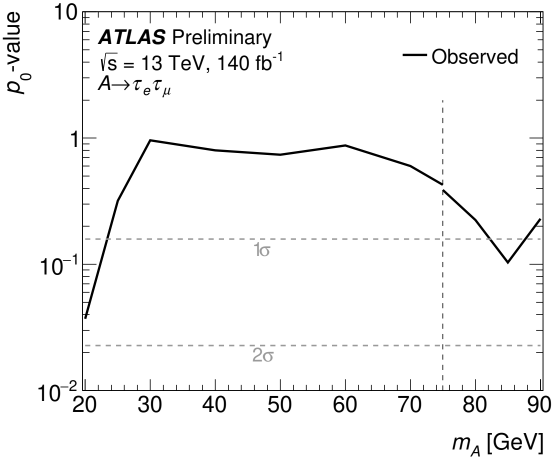

Matrix method in the low-mass $A \to \tau^+\tau^-$ search

for 1 electron (1st index) and 1 muon (2nd index):

$$\begin{pmatrix} N^{\mathrm{TT}}_{\mathrm{XX}} \\ N^{\mathrm{T\bar{T}}}_{\mathrm{XX}} \\ N^{\mathrm{\bar{T}T}}_{\mathrm{XX}} \\ N^{\mathrm{\bar{T}\bar{T}}}_{\mathrm{XX}} \end{pmatrix} = \begin{pmatrix} \varepsilon^e_{\mathrm{real}}\varepsilon^\mu_{\mathrm{real}} & \varepsilon^e_{\mathrm{real}}\varepsilon^\mu_{\mathrm{fake}} & \varepsilon^e_{\mathrm{fake}}\varepsilon^\mu_{\mathrm{real}} & \varepsilon^e_{\mathrm{fake}}\varepsilon^\mu_{\mathrm{fake}} \\ \varepsilon^e_{\mathrm{real}}\bar{\varepsilon}^\mu_{\mathrm{real}} & \varepsilon^e_{\mathrm{real}}\bar{\varepsilon}^\mu_{\mathrm{fake}} & \varepsilon^e_{\mathrm{fake}}\bar{\varepsilon}^\mu_{\mathrm{real}} & \varepsilon^e_{\mathrm{fake}}\bar{\varepsilon}^\mu_{\mathrm{fake}} \\ \bar{\varepsilon}^e_{\mathrm{real}}\varepsilon^\mu_{\mathrm{real}} & \bar{\varepsilon}^e_{\mathrm{real}}\varepsilon^\mu_{\mathrm{fake}} & \bar{\varepsilon}^e_{\mathrm{fake}}\varepsilon^\mu_{\mathrm{real}} & \bar{\varepsilon}^e_{\mathrm{fake}}\varepsilon^\mu_{\mathrm{fake}} \\ \bar{\varepsilon}^e_{\mathrm{real}}\bar{\varepsilon}^\mu_{\mathrm{real}} & \bar{\varepsilon}^e_{\mathrm{real}}\bar{\varepsilon}^\mu_{\mathrm{fake}} & \bar{\varepsilon}^e_{\mathrm{fake}}\bar{\varepsilon}^\mu_{\mathrm{real}} & \bar{\varepsilon}^e_{\mathrm{fake}}\bar{\varepsilon}^\mu_{\mathrm{fake}} \end{pmatrix} \cdot \begin{pmatrix} N^{\mathrm{LL}}_{\mathrm{RR}} \\ N^{\mathrm{LL}}_{\mathrm{RF}} \\ N^{\mathrm{LL}}_{\mathrm{FR}} \\ N^{\mathrm{LL}}_{\mathrm{FF}} \end{pmatrix}$$

$\to$ Inverting matrix gives 3 fake backgrounds:

$$N^{\mathrm{TT}}_{\mathrm{RF,\,est}} = \frac{\varepsilon^e_{\mathrm{real}}\varepsilon^\mu_{\mathrm{fake}}}{(\varepsilon^e_{\mathrm{real}} - \varepsilon^e_{\mathrm{fake}})(\varepsilon^\mu_{\mathrm{real}} - \varepsilon^\mu_{\mathrm{fake}})} \left[-\bar{\varepsilon}^e_{\mathrm{fake}}\bar{\varepsilon}^\mu_{\mathrm{real}} N^{\mathrm{TT}}_{\mathrm{XX}} + \bar{\varepsilon}^e_{\mathrm{fake}}\varepsilon^\mu_{\mathrm{real}} N^{\mathrm{T\bar{T}}}_{\mathrm{XX}} + \varepsilon^e_{\mathrm{fake}}\bar{\varepsilon}^\mu_{\mathrm{real}} N^{\mathrm{\bar{T}T}}_{\mathrm{XX}} - \varepsilon^e_{\mathrm{fake}}\varepsilon^\mu_{\mathrm{real}} N^{\mathrm{\bar{T}\bar{T}}}_{\mathrm{XX}} \right],$$

$$N^{\mathrm{TT}}_{\mathrm{FR,\,est}} = \frac{\varepsilon^e_{\mathrm{fake}}\varepsilon^\mu_{\mathrm{real}}}{(\varepsilon^e_{\mathrm{real}} - \varepsilon^e_{\mathrm{fake}})(\varepsilon^\mu_{\mathrm{real}} - \varepsilon^\mu_{\mathrm{fake}})} \left[-\bar{\varepsilon}^e_{\mathrm{real}}\bar{\varepsilon}^\mu_{\mathrm{fake}} N^{\mathrm{TT}}_{\mathrm{XX}} + \bar{\varepsilon}^e_{\mathrm{real}}\varepsilon^\mu_{\mathrm{fake}} N^{\mathrm{T\bar{T}}}_{\mathrm{XX}} + \varepsilon^e_{\mathrm{real}}\bar{\varepsilon}^\mu_{\mathrm{fake}} N^{\mathrm{\bar{T}T}}_{\mathrm{XX}} - \varepsilon^e_{\mathrm{real}}\varepsilon^\mu_{\mathrm{fake}} N^{\mathrm{\bar{T}\bar{T}}}_{\mathrm{XX}} \right],$$

$$N^{\mathrm{TT}}_{\mathrm{FF,\,est}} = \frac{\varepsilon^e_{\mathrm{fake}}\varepsilon^\mu_{\mathrm{fake}}}{(\varepsilon^e_{\mathrm{real}} - \varepsilon^e_{\mathrm{fake}})(\varepsilon^\mu_{\mathrm{real}} - \varepsilon^\mu_{\mathrm{fake}})} \left[+\bar{\varepsilon}^e_{\mathrm{real}}\bar{\varepsilon}^\mu_{\mathrm{real}} N^{\mathrm{TT}}_{\mathrm{XX}} - \bar{\varepsilon}^e_{\mathrm{real}}\varepsilon^\mu_{\mathrm{real}} N^{\mathrm{T\bar{T}}}_{\mathrm{XX}} - \varepsilon^e_{\mathrm{real}}\bar{\varepsilon}^\mu_{\mathrm{real}} N^{\mathrm{\bar{T}T}}_{\mathrm{XX}} + \varepsilon^e_{\mathrm{real}}\varepsilon^\mu_{\mathrm{real}} N^{\mathrm{\bar{T}\bar{T}}}_{\mathrm{XX}} \right].$$

- Can be converted to event weights via IFF Fake Bkg Tools

Calculation of efficiencies

- Normally: measure assumingly independent $\text{efficiency} = \frac{\#\text{tight leptons}}{\#\text{loose leptons}}$ of each lepton
  $\Rightarrow$ IFF Fake Efficiency Tool
- Here: parametrize one lepton's efficiencies in other lepton's tightness
  $\Rightarrow$ (Fake) leptons no longer assumed to be independent!
- Real efficiencies calculated in SR (and ZCR for non-tight) using MC only

$$\Rightarrow \varepsilon^{e}_{\text{real}}(\mu) = \begin{cases} \frac{N^{\text{TT}}_{\text{RX}}}{N^{\text{LT}}_{\text{RX}}}, & \mu \text{ tight} \\ \frac{N^{\text{T}\overline{\text{T}}}_{\text{RX}}}{N^{\text{L}\overline{\text{T}}}_{\text{RX}}}, & \mu \text{ not tight} \end{cases} \qquad \varepsilon^{\mu}_{\text{real}}(e) = \begin{cases} \frac{N^{\text{TT}}_{\text{XR}}}{N^{\text{TL}}_{\text{XR}}}, & e \text{ tight} \\ \frac{N^{\overline{\text{T}}\text{T}}_{\text{XR}}}{N^{\overline{\text{T}}\text{L}}_{\text{XR}}}, & e \text{ not tight} \end{cases}$$

- Fake efficiencies from FVR, using data, subtracting MC with real lepton

$$\Rightarrow \varepsilon^{e}_{\text{fake}}(\mu) = \begin{cases} \frac{N^{\text{TT}}_{\text{Data}} - N^{\text{TT}}_{\text{RX}}}{N^{\text{LT}}_{\text{Data}} - N^{\text{LT}}_{\text{RX}}}, & \mu \text{ tight} \\ \frac{N^{\text{T}\overline{\text{T}}}_{\text{Data}} - N^{\text{T}\overline{\text{T}}}_{\text{RX}}}{N^{\text{L}\overline{\text{T}}}_{\text{Data}} - N^{\text{L}\overline{\text{T}}}_{\text{RX}}}, & \mu \text{ not tight} \end{cases} \qquad \varepsilon^{\mu}_{\text{fake}}(e) = \begin{cases} \frac{N^{\text{TT}}_{\text{Data}} - N^{\text{TT}}_{\text{XR}}}{N^{\text{TL}}_{\text{Data}} - N^{\text{TL}}_{\text{XR}}}, & e \text{ tight} \\ \frac{N^{\overline{\text{T}}\text{T}}_{\text{Data}} - N^{\overline{\text{T}}\text{T}}_{\text{XR}}}{N^{\overline{\text{T}}\text{L}}_{\text{Data}} - N^{\overline{\text{T}}\text{L}}_{\text{XR}}}, & e \text{ not tight} \end{cases}$$

Calculation of efficiencies

- Same combined e-μ-triggers as in analysis
- Loose ID & Loose isolation vs. Medium ID & Tight isolation
- Efficiencies binned in p_T and tightness of other lepton
- Difference of up to 9% due to tightness parametrization

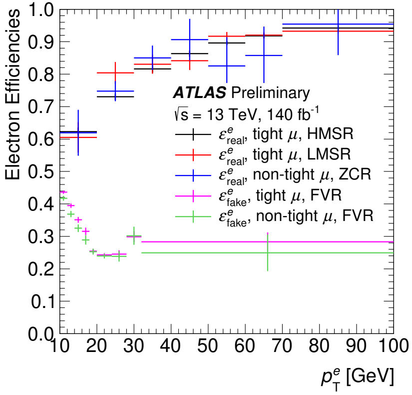

Calculation of efficiencies

- Same combined e-μ-triggers as in analysis
- `Loose` ID & `Loose` isolation vs. `Medium` ID & `Tight` isolation
- Efficiencies binned in p_T and tightness of other lepton
- Difference of up to 9% due to tightness parametrization

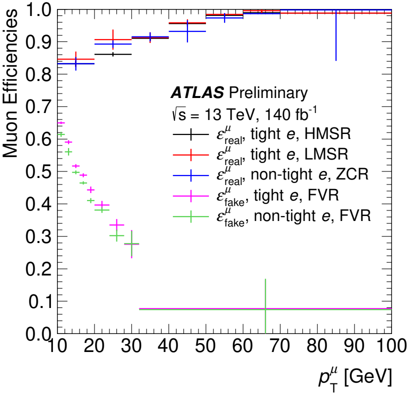

$Z \to \tau^+\tau^-$ reweighting

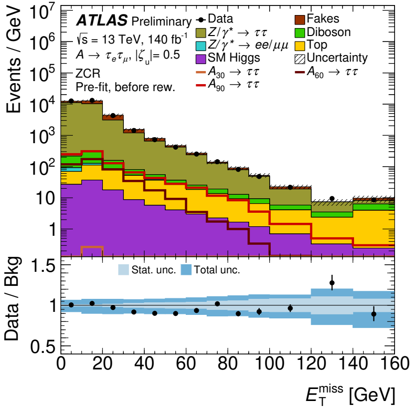

E_T^{miss} in $Z \to \tau\tau$ CR before reweighting

$\Rightarrow$

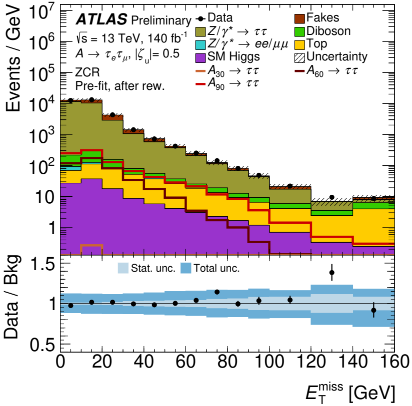

E_T^{miss} in $Z \to \tau\tau$ CR after reweighting

$Z \to \tau^+\tau^-$ reweighting

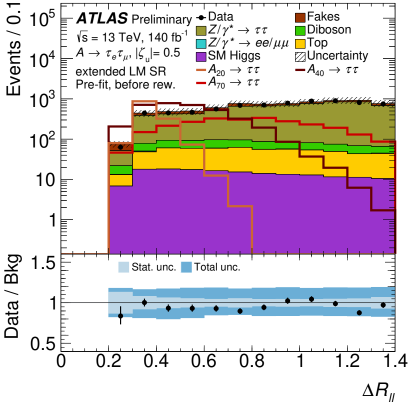

$\Delta R_{\ell\ell}$ in extended low-mass SR before reweighting

$\Rightarrow$

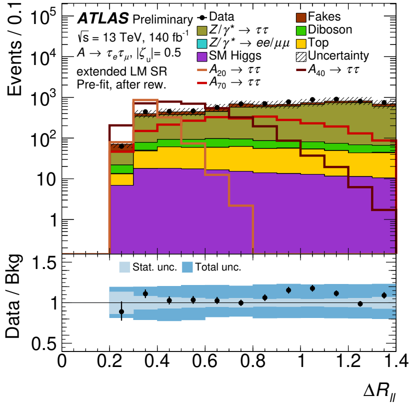

$\Delta R_{\ell\ell}$ in extended low-mass SR after reweighting

Signal region – p_T^A distribution

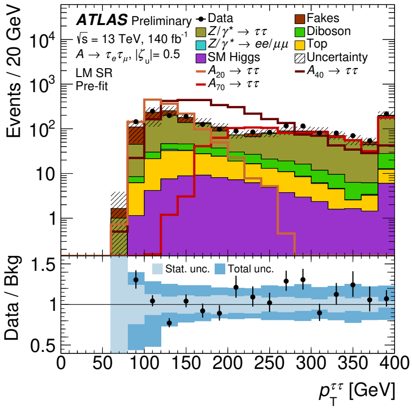

p_T^{Higgs} in the low-mass SR

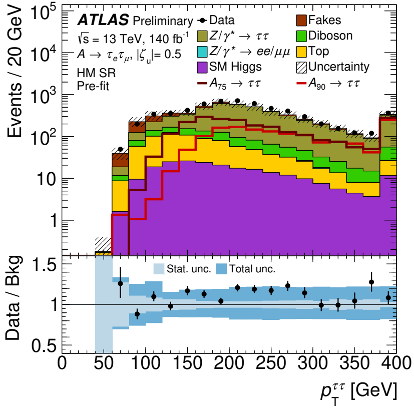

p_T^{Higgs} in the high-mass SR

$Z \to \tau\tau$ CR – prefit and postfit distribution

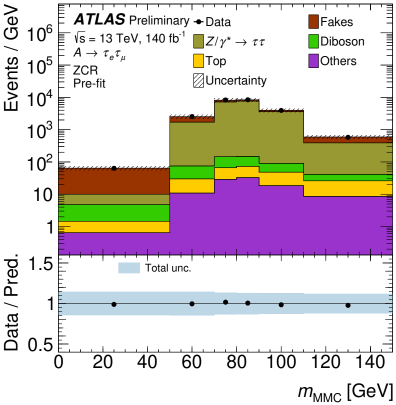

$\Rightarrow$

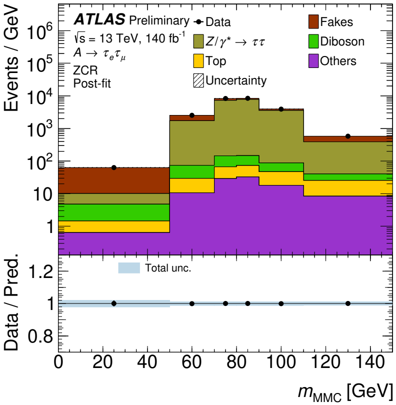

Top CR – prefit and postfit distribution

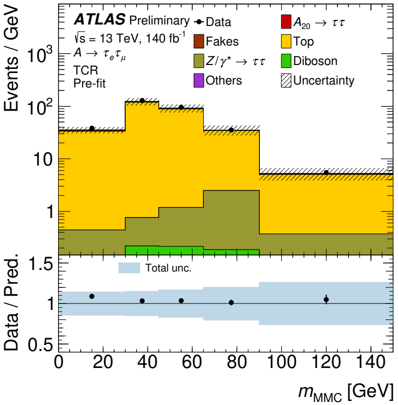

$\Longrightarrow$

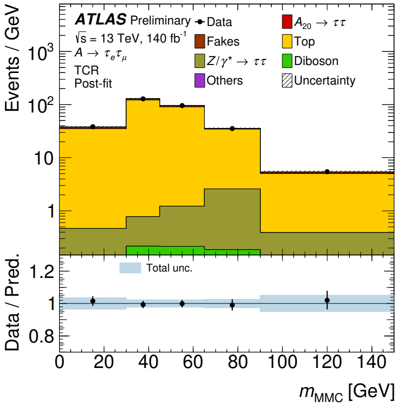

Event yields

	ZCR	FVR	TCR	low-mass SR	high-mass SR
Fakes	$59\,680 \pm 690$ (18%)	$44\,850 \pm 430$ (97%)	213 ± 50 (3.5%)	316 ± 45 (17%)	495 ± 55 (9.0%)
$Z/\gamma^* \to \tau^+\tau^-$	$262\,700 \pm 1800$ (79%)	82 ± 27 (0.18%)	116.1 ± 4.0 (1.9%)	1210 ± 36 (63%)	3701 ± 46 (67%)
Diboson	4552 ± 26 (1.4%)	747.3 ± 7.4 (1.6%)	10.82 ± 0.50 (0.18%)	139.1 ± 2.4 (7.3%)	449.2 ± 4.4 (8.2%)
$Z/\gamma^* \to \ell^+\ell^-$	468 ± 71 (0.14%)	354 ± 68 (0.77%)	0.28 ± 0.12 ($< 0.1\%$)	4.0 ± 1.7 (0.21%)	9.8 ± 3.3 (0.18%)
Top	3327 ± 22 (1.0%)	2.02 ± 0.51 ($< 0.1\%$)	5653 ± 28 (94%)	162.9 ± 4.7 (8.5%)	611.4 ± 9.3 (11%)
SM Higgs	1108.7 ± 2.6 (0.33%)	3.63 ± 0.18 ($< 0.1\%$)	5.79 ± 0.23 (0.097%)	76.86 ± 0.79 (4.0%)	227.4 ± 1.3 (4.1%)
total Bkg	$331\,800 \pm 2000$	$46\,040 \pm 440$	5999 ± 57	1908 ± 58	5494 ± 73
Data	331 797	44 587	6227	1987	6119

$\Rightarrow$ Values in brackets show relative contributions